Supplementary Information: Simulation of intercalation and phase transitions in nano-porous, polycrystalline agglomerates

Simon Daubner[1,2*], Marcel Weichel[2], Martin Reder[2,3], Daniel Schneider[2,3],
Qi Huang[4], Alexander E. Cohen[5], Martin Z. Bazant[5], Britta Nestler[2,3]

[1]Dyson School of Design Engineering, Imperial College London, London, UK.
[2]Institute for Applied Materials (IAM-MMS), Karlsruhe Institute of Technology, Karlsruhe, Germany.
[3]Institute for Digital Materials Science (IDM), Karlsruhe University of Applied Sciences, Karlsruhe, Germany.
[4]State Key Lab of Powder Metallurgy, Central South University, Changsha, China.
[5]Department of Chemical Engineering, Massachusetts Institute of Technology, Cambridge, USA.

1 Supplementary Results: Analytical considerations for the MP-SBM

While the Cahn-Hilliard equation has often been employed for the simulation of intercalation into lithium iron phosphate (LFP) [1–3], the potential of multiphase-field approaches for the simulation of agglomerated particles [4] and materials which undergo multiple phase transitions during cycling [5] has been highlighted in our previous works. An extension of the smooth boundary concept to multi-phase systems is necessary to generalize the proposed simulation framework for arbitrary particle morphologies. As discussed in our previous work [6], the phase transition within an LFP particle can be modelled employing a multiphase-field approach based on an Allen-Cahn evolution equation coupled with mass conservation given by the evolution of the chemical potential [7]. This three phase system (electrolyte, FP and LFP) is an ideal starting point for the validation of the MP-SBM and a subsequent generalization to multi-phase systems. The first order phase transformation (LP→LFP) can be described through the evolution of a single order parameter φ which denotes the LFP volume fraction. From Eq. 5 in the main manuscript we derive

$$\frac{\partial \varphi}{\partial t} = -M_{\alpha\beta}\left(-\gamma_{\alpha\beta}\boldsymbol{\nabla}^2\varphi + \frac{8\gamma_{\alpha\beta}}{\varepsilon^2\pi^2}(1-2\varphi) + |\boldsymbol{\nabla}\varphi|\left(\Delta^{\alpha\beta}_{\text{chem}}\right)\right)$$

where $|\boldsymbol{\nabla}\varphi|$ can be approximated as $|\boldsymbol{\nabla}\varphi| \approx \frac{4}{\varepsilon\pi}\sqrt{\varphi(1-\varphi)}$ and the chemical driving force is given as $\Delta^{\alpha\beta}_{\text{chem}} = (f^{\text{LFP}}_{\text{chem}} - \mu_{\text{Li}}c^{\text{LFP}}_{\text{Li}}) - (f^{\text{FP}}_{\text{chem}} - \mu_{\text{Li}}c^{\text{FP}}_{\text{Li}})$. Note that all following considerations can be equally made for the well-potential where $\partial f_{\text{well}}/\partial\varphi = 2\frac{9\gamma_{\alpha\beta}}{\varepsilon}\varphi(1-2\varphi)(1-\varphi)$ and $|\boldsymbol{\nabla}\varphi| \approx \frac{3}{\varepsilon}\varphi(1-\varphi)$. From Eq. 9 in the main manuscript, we derive the coupled evolution equation of the chemical potential of intercalated ions

$$\frac{\partial \mu}{\partial t} = \left[\frac{\partial c^\alpha}{\partial \mu}\varphi + \frac{\partial c^\beta}{\partial \mu}(1-\varphi)\right]^{-1} \left(\boldsymbol{\nabla}\cdot(\mathbb{M}\boldsymbol{\nabla}\mu) + R_{\text{bulk}} - (c^\alpha - c^\beta)\frac{\partial \varphi}{\partial t}\right).$$

The ion mobility $\mathbb{M} = (\mathbb{D}^\alpha \frac{\partial c^\alpha}{\partial \mu}\varphi + \mathbb{D}^\beta \frac{\partial c^\beta}{\partial \mu}(1-\varphi)$ is defined by linear interpolation of the phase-inherent mobilities. To compute the phase transition within a given particle geometry which is parametrized by the indicator function ψ, we re-write the problem as

$$\begin{aligned}\psi\frac{\partial \varphi}{\partial t} = -\frac{M_{\alpha\beta}}{2\varepsilon}\Big[&-2\varepsilon\gamma_{\alpha\beta}\boldsymbol{\nabla}\cdot(\psi\boldsymbol{\nabla}\varphi) + 2\varepsilon\gamma_{\alpha\beta}\boldsymbol{\nabla}\psi\cdot\boldsymbol{\nabla}\varphi \\ &+ \frac{16\gamma_{\alpha\beta}}{\varepsilon\pi^2}(\psi - 2\psi\varphi) + 2\varepsilon\psi|\boldsymbol{\nabla}\varphi|\left(\Delta^{\alpha\beta}_{\text{chem}}\right)\Big].\end{aligned} \tag{1}$$

The term $\boldsymbol{\nabla}\psi\cdot\boldsymbol{\nabla}\varphi$ imposes the wetting angle condition and is assumed to be zero in the following. The concentration evolution equation can be re-written as

$$\frac{\partial c}{\partial t} = \frac{1}{\psi}\boldsymbol{\nabla}\cdot(\psi\mathbb{M}(\varphi)\boldsymbol{\nabla}\mu) + \frac{|\boldsymbol{\nabla}\psi|}{\psi}J_N + R_{\text{bulk}}.$$

Employing $\frac{\partial c}{\partial t} = ((\partial c^\alpha/\partial\mu)\varphi - (\partial c^\beta/\mu)(1-\varphi))\frac{\partial \mu}{\partial t} + (c^\alpha - c^\beta)\frac{\partial \varphi}{\partial t}$, this results in

$$\frac{\partial \mu}{\partial t} = \left[\frac{\partial c^\alpha}{\partial \mu}\varphi + \frac{\partial c^\beta}{\partial \mu}(1-\varphi)\right]^{-1} \left(\frac{1}{\psi}\boldsymbol{\nabla}\cdot(\psi\mathbb{M}(\varphi)\boldsymbol{\nabla}\mu) + \frac{|\boldsymbol{\nabla}\psi|}{\psi}J_N + R_{\text{bulk}} - (c^\alpha - c^\beta)\frac{\partial \varphi}{\partial t}\right) \tag{2}$$

where $|\boldsymbol{\nabla}\psi|J_N$ defines the flux boundary condition. This set of equations corresponds to the coupled evolution of φ and μ everywhere in the domain, while ψ marks the region of interest as sketched in Figure 2 a).

We now reformulate Eq. (1) and (2) in terms of the multi-phase field perspective shown in Figure 2 b). The three phase variables ϕ_α, ϕ_β and ϕ_γ denote volume fractions and, therefore, must fulfill the Gibbs simplex constraint, i.e. $\sum_{\alpha=1}^{N}\phi_\alpha = 1$ and $0 \leq \phi_\alpha$ for all phases α. The electrolyte region is given by $\phi_\gamma = 1 - \psi$ while the active material is given by $\phi_\alpha + \phi_\beta = \psi$. Therefore, the following relation between volume fractions can be derived

$$\phi_\alpha = \frac{V_\alpha}{V} = \frac{V_\alpha}{V_{\text{active}}}\frac{V_{\text{active}}}{V} = \varphi\psi \quad \text{and thus} \quad \frac{\partial \phi_\alpha}{\partial t} = \psi\frac{\partial \varphi}{\partial t}. \tag{3}$$

As we restrict the evolution of the electrolyte-electrode interface, the evolution of phase variables fulfills

$$\frac{\partial \phi_\gamma}{\partial t} = 0 \quad \text{and thus} \quad \frac{\partial \phi_\alpha}{\partial t} = -\frac{\partial \phi_\beta}{\partial t}.$$

We start from a general form of the multiphase-field equations based on the two interfacial energy contributions

$$f_{\text{grad}} = -\varepsilon\sum_{\alpha}\sum_{\beta>\alpha}\gamma_{\alpha\beta}\boldsymbol{\nabla}\phi_\alpha\cdot\boldsymbol{\nabla}\phi_\beta \quad \text{and} \quad f_{\text{pot}} = \frac{16}{\varepsilon\pi^2}\sum_{\alpha}\sum_{\beta>\alpha}\gamma_{\alpha\beta}\phi_\alpha\phi_\beta \tag{4}$$

where we employ the multi-obstacle potential in accordance with [8]. As ϕ_γ does not evolve over time, we set the phase mobilities $M_{\alpha\gamma} = M_{\beta\gamma} = 0$. Furthermore, the pairwise interfacial energies with respect to the electrolyte phase are assumed to have the same value $\gamma_{\alpha\gamma} = \gamma_{\beta\gamma}$ which corresponds to the formation of 90° angles of the $\alpha\beta$-interface with respect to the particle boundary. With these assumptions, the evolution equation reads

$$\frac{\partial \phi_\alpha}{\partial t} = -\frac{M_{\alpha\beta}}{2\varepsilon}\left(\varepsilon\gamma_{\alpha\beta}\left(\boldsymbol{\nabla}^2\phi_\beta - \boldsymbol{\nabla}^2\phi_\alpha\right) + \frac{16}{\varepsilon\pi^2}\gamma_{\alpha\beta}(\phi_\beta-\phi_\alpha) + \frac{8}{\pi}\sqrt{\phi_\alpha\phi_\beta}\Delta^{\alpha\beta}_{\text{chem}}\right). \tag{5}$$

Eq. (1) can be expressed in terms of ϕ_α and ϕ_β using the relations in Eq. (3), which yields

$$\psi\frac{\partial\varphi}{\partial t} = \frac{\partial \phi_\alpha}{\partial t} = -\frac{M_{\alpha\beta}}{2\varepsilon}\left(\frac{\varepsilon\gamma_{\alpha\beta}}{\phi_\alpha+\phi_\beta}\left(\phi_\alpha\boldsymbol{\nabla}^2\phi_\beta - \phi_\beta\boldsymbol{\nabla}^2\phi_\alpha\right) + \frac{16}{\varepsilon\pi^2}\gamma_{\alpha\beta}(\phi_\beta-\phi_\alpha) + \frac{8}{\pi}\sqrt{\phi_\alpha\phi_\beta}\Delta^{\alpha\beta}_{\text{chem}}\right).$$

The comparison with the multiphase-field approach in Eq. (5) shows that the last two terms are identical due their linearity while the laplace terms differ slightly. For $\phi_\gamma = 0$ and thus $\phi_\alpha+\phi_\beta = 1$ and $\boldsymbol{\nabla}\phi_\beta = -\boldsymbol{\nabla}\phi_\alpha$ both evolution equations become identical which means the bulk behaviour is identical while triple junction dynamics might differ.

Similarly, Eq. (2) for the chemical potential can be re-written employing $\varphi = \phi_\alpha/\psi$ and $(1-\varphi) = \phi_\beta/\psi$ which results in

$$\begin{aligned}\frac{\partial\mu}{\partial t} &= \left[\frac{\partial c^\alpha}{\partial\mu}\frac{\phi_\alpha}{\psi} + \frac{\partial c^\beta}{\partial\mu}\frac{\phi_\beta}{\psi}\right]^{-1}\left(\frac{1}{\psi}\boldsymbol{\nabla}\cdot\left(\psi\mathbb{M}\left(\frac{\phi_\alpha}{\psi}\right)\boldsymbol{\nabla}\mu\right) + \frac{|\boldsymbol{\nabla}\psi|}{\psi}J_N + R_{\text{bulk}} - (c^\alpha - c^\beta)\frac{1}{\psi}\frac{\partial\phi_\alpha}{\partial t}\right)\\ &= \left[\frac{\partial c^\alpha}{\partial\mu}\phi_\alpha + \frac{\partial c^\beta}{\partial\mu}\phi_\beta\right]^{-1}\left(\boldsymbol{\nabla}\cdot\left(\psi\mathbb{M}\left(\frac{\phi_\alpha}{\psi}\right)\boldsymbol{\nabla}\mu\right) + |\boldsymbol{\nabla}\psi|J_N + \psi R_{\text{bulk}} - (c^\alpha - c^\beta)\frac{\partial\phi_\alpha}{\partial t}\right).\end{aligned}$$

The ion mobility is then given by $\psi\mathbb{M} = \mathbb{D}^\alpha\frac{\partial c^\alpha}{\partial\mu}\phi_\alpha + \mathbb{D}^\beta\frac{\partial c^\beta}{\partial\mu}\phi_\beta$. This can be generalized for a multiphase system with N phases if we introduce the two subsets of inactive material $\phi_0 = \sum_{\alpha=0}^{A-1}\phi_\alpha$ and active material $\psi = \sum_{\alpha=A}^{N}\phi_\alpha$ and, thus

$$\frac{\partial\mu}{\partial t} = \left[\sum_{\alpha=A}^{N}\frac{\partial c^\alpha}{\partial\mu}\phi_\alpha\right]^{-1}\left[\boldsymbol{\nabla}\cdot\left(\left(\sum_{\alpha=A}^{N}D^\alpha\frac{\partial c^\alpha}{\partial\mu}\phi_\alpha\right)\boldsymbol{\nabla}\mu\right) + |\boldsymbol{\nabla}\psi|J_N + \psi R_{\text{bulk}} - \sum_{\alpha=A}^{N}c^\alpha\frac{\partial\phi_\alpha}{\partial t}\right]. \tag{6}$$

This is equivalent to defining the concentration in the active material as $c_{\text{active}} = (\sum_{\alpha=A}^{N}c^\alpha\phi_\alpha)/\psi$.

2 Supplementary Note: Simulation validation

From the considerations above, it becomes clear that both approaches yield almost identical evolution equations for the first-order phase transformation and the coupled chemical potential. Deviations of the field solutions are expected at the diffuse boundary due to the differences in laplace terms (i.e. in triple junctions in the MPF approach). The important difference is that the second approach (MP-SBM, compare Fig. 2 b) in main manuscript) is directly compatible with most existing multiphase-field formulations and can be easily implemented for an arbitrary amount of phases.

For validation, we employ an ellipsoid particle under galvanostatic boundary conditions. An initial patch of the high-concentration phase will grow due to the continued intercalation reaction (see Fig. 1a). Note that the surface fluxes are locally varying while the integral fulfills the constraint of a constant C-rate according to Eq. 12 in the main manuscript. As the concentration increases spontaneous phase nucleation occurs at the right side of the particle as shown in Figure 1 b). The first simulation is based on the standard smooth boundary derivation (SBM), i.e. Equations (1) and (2). The corresponding temporal evolution of concentration is shown in Figure 1b. The second simulation is based on the extended multi-phase smooth boundary method (MP-SBM) given by Equations (5) and (6). The difference of concentration fields between both approaches is shown in Figure 1 c). The comparison of concentration fields in Figure 1 c) reveals that the interface motion of the high-concentration phase is almost identical in the initial timesteps with small deviations around the triple junction. As the diffuse boundary influences the nucleation behaviour, larger differences arise later during the simulation when another patch of ϕ_α nucleates at the right side of the ellipse. Nucleation is more likely to happen where the curvature of ψ is higher [9], which can be observed in both simulations.

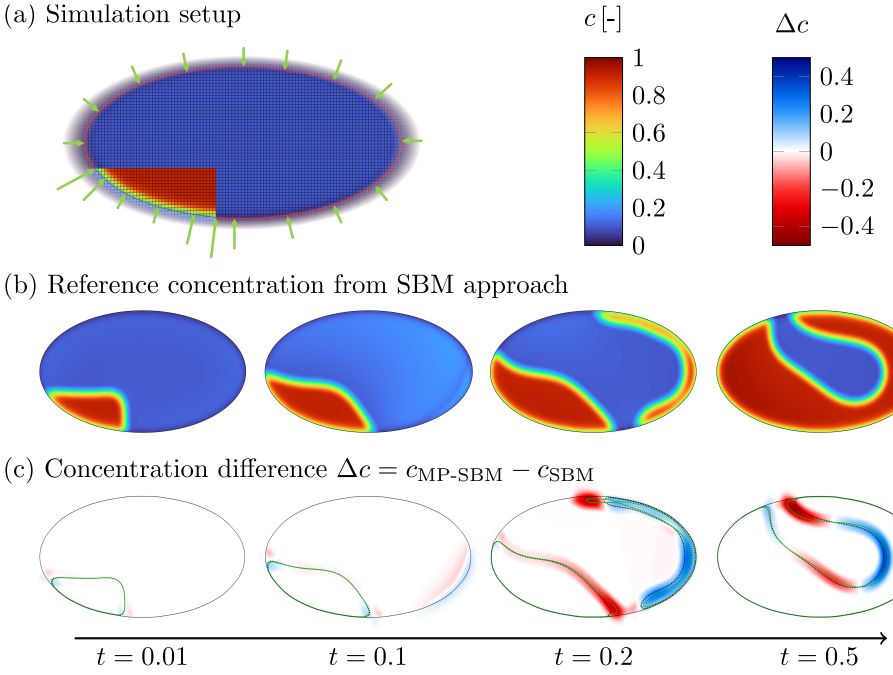

Figure 1: Comparison of the concentration evolution in an ellipsoid particle with constant current intercalation boundary fluxes as sketched in a). The reference solution based on the SBM approach (compare Fig. 1 a) main manuscript) is shown in b). Growth of the existing high-concentration area as well as nucleation at the high curvature area to the right can be observed. The same simulation has been carried out with the MP-SBM approach (compare Fig. 1 b) main manuscript) and the difference of concentration fields in shown in c). The black dotted line denotes the $c_{\text{SBM}} = 0.5$ isoline while the $c_{\text{MP-SBM}} = 0.5$ isoline is shown in green for comparison.

References

[1] Huttin, M., Kamlah, M.: Phase-field modeling of stress generation in electrode particles of lithium ion batteries. Applied Physics Letters **101**(13) (2012) https://doi.org/10.1063/1.4754705

[2] Zhao, Y., Stein, P., Xu, B.-X.: Isogeometric analysis of mechanically coupled Cahn–Hilliard phase segregation in hyperelastic electrodes of Li-ion batteries. Computer Methods in Applied Mechanics and Engineering **297**, 325–347 (2015) https://doi.org/10.1016/j.cma.2015.09.008

[3] Hong, L., Li, L., Chen-Wiegart, Y.-K., Wang, J., Xiang, K., Gan, L., Li, W., Meng, F., Wang, F., Wang, J., Chiang, Y.-M., Jin, S., Tang, M.: Two-dimensional lithium diffusion behavior and probable hybrid phase transformation kinetics in olivine lithium iron phosphate. Nature Communications **8**(1), 1194 (2017) https://doi.org/10.1038/s41467-017-01315-8

[4] Daubner, S., Weichel, M., Hoffrogge, P.W., Schneider, D., Nestler, B.: Modeling Anisotropic Transport in Polycrystalline Battery Materials. Batteries **9**(6), 310 (2023) https://doi.org/10.3390/batteries9060310

[5] Daubner, S., Dillenz, M., Pfeiffer, L.F., Gauckler, C., Rosin, M., Burgard, N., Martin, J., Axmann, P., Sotoudeh, M., Groß, A., Schneider, D., Nestler, B.: Combined study of phase transitions in the P2-type NaXNi1/3Mn2/3O2 cathode material: experimental, ab-initio and multiphase-field results. npj Computational Materials **10**(1), 75 (2024) https://doi.org/10.1038/s41524-024-01258-x

[6] Daubner, S., Kubendran Amos, P.G., Schoof, E., Santoki, J., Schneider, D., Nestler, B.: Multiphase-field modeling of spinodal decomposition during intercalation in an Allen-Cahn framework. Physical Review Materials **5**(3), 035406 (2021) https://doi.org/10.1103/PhysRevMaterials.5.035406

[7] Choudhury, A., Nestler, B.: Grand-potential formulation for multicomponent phase transformations combined with thin-interface asymptotics of the double-obstacle potential. Physical Review E **85**(2), 021602 (2012) https://doi.org/10.1103/PhysRevE.85.021602

[8] Daubner, S., Weichel, M., Schneider, D., Nestler, B.: Modeling intercalation in cathode materials with phase-field methods: Assumptions and implications using the example of LiFePO4. Electrochimica Acta **421**(May), 140516 (2022) https://doi.org/10.1016/j.electacta.2022.140516

[9] Santoki, J., Kamlah, M., Schneider, D., Nestler, B., Selzer, M., Wang, F.: Phase-field study of surface irregularities of a cathode particle during intercalation. Modelling and Simulation in Materials Science and Engineering **26**(6), 065013 (2018) https://doi.org/10.1088/1361-651x/aad20a